

Suitability of carbon nanotubes grown by chemical vapor deposition for electrical devices

B. Babić, J. Furer, M. Iqbal and C. Schönenberger

Institut für Physik, Universität Basel, Klingelbergstr. 82, CH-4056 Basel, Switzerland

Abstract. Using carbon nanotubes (CNTs) produced by chemical vapor deposition, we have explored different strategies for the preparation of carbon nanotube devices suited for electrical and mechanical measurements. Though the target device is a single small diameter CNT, there is compelling evidence for bundling, both for CNTs grown over structured slits and on rigid supports. Whereas the bundling is substantial in the former case, individual single-wall CNTs (SWNTs) can be found in the latter. Our evidence stems from mechanical and electrical measurements on contacted tubes. Furthermore, we report on the fabrication of low-ohmic contacts to SWNTs. We compare Au, Ti and Pd contacts and find that Pd yields the best results.

The present work is structured in two main sections. The first is devoted to our results on carbon nanotubes (CNTs) grown by chemical vapor deposition (CVD) emphasizing on the problem of CNT bundling, which occurs during growth. The second section discusses our results on the contacting of CVD-grown tubes using the metals Au, Ti and Pd.

SUPPORTED AND SUSPENDED CARBON NANOTUBES PREPARED BY CVD

The full control and understanding of structural and electronic properties of carbon nanotubes remain a major challenge towards their applications in nanoelectronics. Today, there exists several different production methods of carbon nanotubes (CNTs). Among them, chemical vapor deposition (CVD) emerged [1, 2, 3] as the most prominent one for the investigation of the electronic and electromechanical properties of CNTs. The most important advantages of the CVD method are that CNTs can be grown at specific locations on the substrate and at lower temperatures with simpler equipments as compared to the arc discharge and laser ablation methods. However, CNTs grown with this method vary in a quality and display a rather large dispersion in diameter which might be a severe problem for potential applications. Following the published recipes, we found that CVD grown CNTs differ dramatically if they are grown supported on a substrate or suspended over structured slits. This suggests that the nanotube-substrate interaction plays an important role in the final product in addition to growth parameters and catalysts.

Growth method

Two types of catalysts are used for the growth of CNTs. The first catalyst, which we will name catalyst 1, is similar to that described in Ref. [2]. The catalyst suspension consists of 1 mg iron nitrate seeds ($\text{Fe}(\text{NO}_3)_3 \cdot 9\text{H}_2\text{O}$) dissolved in 10 ml of isopropanol. The other catalyst, which we will call in the rest of the paper catalyst 2, has been prepared similar to that described in Ref. [3]. To 15 ml of methanol, 15 mg alumina oxide, 20 mg $\text{Fe}(\text{NO}_3)_3 \cdot 9\text{H}_2\text{O}$ and 5 mg $\text{MoO}_2(\text{acac})_2$ are added. Both suspensions are sonicated for 1 hour, stirred overnight and sonicated every time for at least 20 min before deposition on the substrate [5]. A drop of the suspension is placed on a bare substrate surface or on a substrate with predefined structured areas by electron-beam lithography (EBL) or optical lithography in the corresponding resist. After spinning at 2000 r.p.m for 40 sec, the substrate is baked at 150 °C for 5 min, followed by lift-off. The CVD growth of CNTs is performed in a quartz-tube furnace between 750 – 1000 °C at atmospheric pressure using different gases. For catalyst 1 we used a mixture of either ethylene or methane with hydrogen and argon with respective flow rates of 2, 400, and 600 cm^3/min [4]. For the catalyst 2, we have used a mixture of methane and argon with respective flow rates of 5000 and 1000 cm^3/min [4]. During heating and cooling of the furnace, the quartz tube is continuously flashed with argon to reduce the contamination of the CNTs and to avoid burning them once they are produced.

Results and Discussion

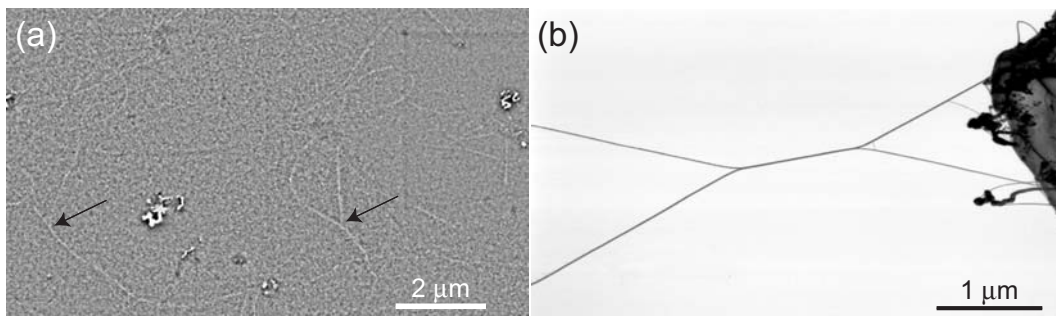


FIGURE 1. SEM images of CNTs grown from catalyst 1. In (a) the CNTs were grown on a Si/SiO₂ substrate at $T=800\text{ }^\circ\text{C}$. The arrows point to visible branches. (b) Typical CNT network, grown over structured slits at $T=750\text{ }^\circ\text{C}$. Note, that CNTs can bridge very large distances.

Carbon nanotubes which are grown at the same temperature but with the two mentioned catalysts on thermally oxidized silicon substrates show similar characteristics. In both cases there is a profound temperature dependence. At relatively low temperatures (750-850 °C) predominantly individual MWNTs or ropes of SWNTs are obtained with high yield. At intermediate temperatures (850-975 °C) individual SWNTs are grown with a typical diameter of 2 nm or thin bundles of SWNTs, but with less yield than at lower temperatures. At high temperatures (>1000 °C), the substrate and the CNTs are often found to be covered with an additional material, which is most likely amorphous carbon. Carbon nanotubes used in transport measurements have been solely produced

at the intermediate temperature range. Fig. 1a shows a scanning electron microscope (SEM) image of CNTs grown from catalyst 1 on a Si/SiO₂ substrate.

For the purpose of mechanical and electromechanical studies, CNTs have been grown over structured slits patterned in Si₃N₄, an example of the outcome is shown in Fig. 1b. It is expected that for sufficiently long CNTs thermal vibrations should be readily observed with transmission and scanning-electron microscopy (TEM and SEM) [6, 7, 8]. This holds only, however, for ‘small’ diameter tubes, because the vibration amplitude is strongly reduced with increasing diameter d according to ($\sim 1/d^2$). Only individual SWNTs are expected to show a substantial vibration amplitude which could be observed in SEM. We suggest this as a simple check to distinguish individual from bundled SWNTs. Fig. 1b shows a representing SEM image of suspended CNTs spanning over long distances ($L > 1 \mu\text{m}$). None of the visible ‘strings’ display observable vibrations. This is not surprising considering the observed CNT branches. Clearly, in this case the CNTs must be bundled. This bundling increases the wider the slit is resulting into complex (but marvellous looking) spider webs. Further details on the search for vibrating suspended tubes can be found in Ref. [8]. We argue that in the absence of a support and at the relatively high temperature CNTs may meet each other during growth. The likelihood is increased if growth proceeds in ‘free’ space over a large distance. Once they touch each other they stick together due to the van der Waals interaction leading to a bundle.

In contrast, the growth on a substrate is different, as the tubes interact with the substrate rather than with each other. Hence, bundling is expected to be reduced. This is confirmed in AFM images, provided the catalyst density is low. However, there are bundles as well, which is evident from the observed branches visible in the AFM image of Fig. 1a (arrows). Even at locations where bundling is not apparent, one can still not be sure that such a nanotube section corresponds to a single-wall tube. Usually this is checked by measuring the height in AFM, but this can be misleading too, because the diameters of CVD-tubes can vary a lot, over 1 – 5 nm as reported by Ref. [9]. We confirm this with our own measurements. Further insight into the question of bundling of CVD-grown CNTs can be obtained from electrical characterizations, which we report next.

Carbon nanotube devices

We have produced CNT devices on chip following two strategies. In the first method the substrate is covered with a layer of polymethylmethacrylate (PMMA) in which windows are patterned by electron-beam lithography (EBL). Next, the catalyst is spread from solution over these patterned structures, after which the PMMA is removed with acetone, leaving isolated catalyst islands ($5 \times 10 \mu\text{m}^2$) on the surface. The substrate with the catalyst is then transferred to the oven where CVD growth of CNTs is performed. From the catalyst islands, CNTs grow randomly in all directions, but because of the relatively large distance between the islands ($5 \mu\text{m}$) just one or a few CNTs bridge them usually. An atomic force microscope (AFM) image in phase mode with several CNTs growing from the catalyst islands is shown in Fig. 2a. An individual SWNT bridging the

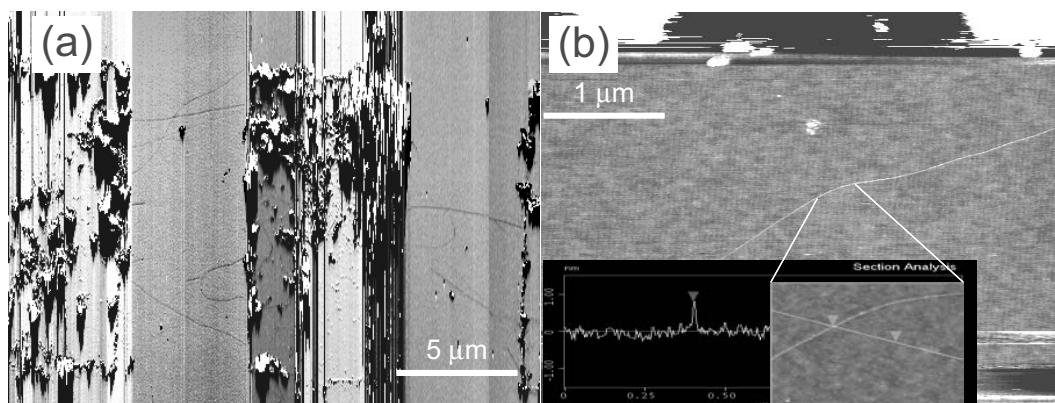


FIGURE 2. (a) Phase image recorded by tapping mode AFM, showing CNTs grown from the patterned catalyst islands and bridging between islands. (b) Topography image of an individual SWNT grown between the catalyst islands recorded by tapping mode AFM. Inset: Height measurement on the line cut (white line) for the SWNT shown in (b). The height measurements yield for the diameter $d = (1.2 \pm 0.2)$ nm for this particular tube.

catalyst islands is shown in Fig. 2b. Metal electrodes (Au, Ti, Pd) are patterned over the catalyst islands with EBL, followed by evaporation and lift-off. The alignments during the EBL structuring have been done corresponding to chromium markers [10]. SEM and AFM images of contacted individual CNTs are shown in Fig. 3a and 3b.

In the second method we spread the (diluted) catalyst over the entire substrate at low concentration. The density is chosen such that at least one CNT grows inside a window of size $10 \times 10 \mu\text{m}^2$. After the CVD process a set of recognizable metallic markers (Ti/Au bilayer) are patterned, again by EBL, see Fig. 3c. Using AFM in tapping mode, a suitable CNT with an apparent height of less than 3 nm is located with respect to the markers. In the final lithography step, electrodes to the selected CNT are patterned by lift-off.

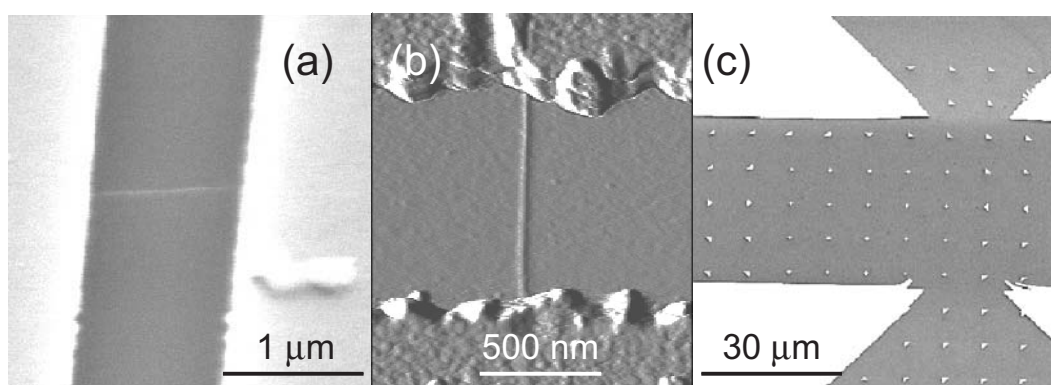


FIGURE 3. (a) SEM image of a SWNT contacted with a Ti/Au bilayer. (b) AFM image recorded in tapping mode of a contacted individual SWNT. (c) SEM image of a set of Ti/Au markers which are used to register the contact structure to the SWNTs selected before by AFM.

Room temperature characterization

Once the samples are made, it is common practice to distinguish semiconducting and metallic CNTs by the dependence of their electrical conductance (G) on the gate voltage (V_g), measured at room temperature ($T \approx 300$ K). This, however, cannot be considered as a proof that an individual SWNT has been contacted, because it is not well understood how the linear response conductance is altered if more than one tube is contributing to electrical transport. Even if measurements were performed on ropes of SWNTs, the measured signatures agreed quite well with the behavior expected for a SWNT [11, 12, 13]. This has been attributed to a dominant electrode-CNT coupling to one nanotube only. This scenario may be true in exceptional cases, but one would expect that the majority of measurements should display signatures that arise from the presence of more than one tube. We have recently observed Fano resonances which we attribute to the interference of a SWNT which is strongly coupled to the electrodes with other more weakly coupled ones [14].

Assuming that all chiralities have equal probability to be formed in growth, $2/3$ of the SWNTs are expected to be semiconducting and $1/3$ metallic. From the measured response of the electrical conductance to the gate voltage (back-gate), $\approx 60\%$ of the devices display metallic (the conductance does not depend on the gate voltage) and $\approx 40\%$ semiconducting behavior. Based on our assumption the larger fraction of metallic gate responses points to the presence of bundles or multishell tubes. If there are on average 2 or 3 tubes per bundle, which are coupled to the electrodes approximately equally, the probability to observe a semiconducting characteristic would amount to $(2/3)^2 = 44\%$ or $(2/3)^3 = 30\%$. Hence, we can conclude that the bundle size is very likely small and close to 2 on average.

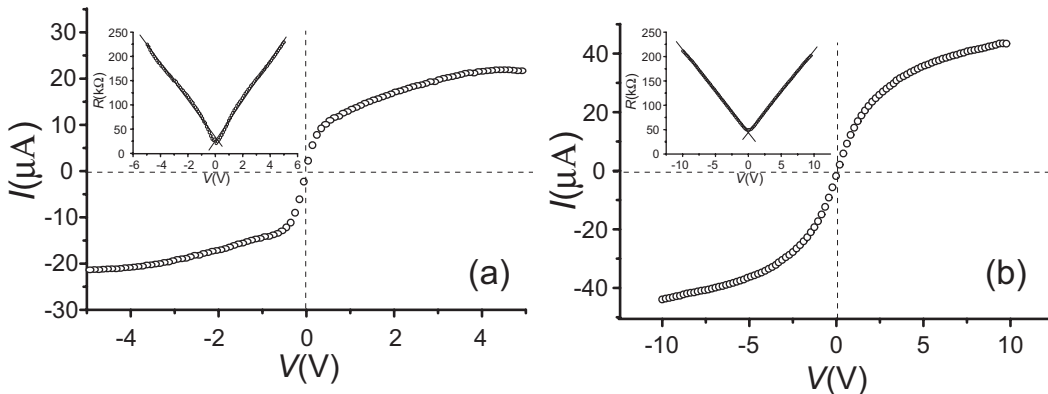


FIGURE 4. Typical $I - V$ characteristics at high bias voltage for CNT samples with a contact spacing of $1 \mu\text{m}$. The insets show $R \equiv V/I$ versus V and fits to Eq. 1 for positive and negative V (lines). (a) The extracted mean value for the saturation current for this device is $I_0 = 24.3 \pm 1.2 \mu\text{A}$ which suggests transport through an individual SWNT. (b) A higher saturation current of $I_0 = 59.3 \pm 2.1 \mu\text{A}$ is found in this device suggesting transport through 2 – 3 CNT shells.

A powerful method to characterize contacted CNTs is to perform transport measurements in the nonlinear transport regime (high bias). As previously reported by Yao *et al.* [15] the emission of zone-boundary or optical phonons is very effective in CNTs at high fields. This effect leads to a saturation of the current for an individual SWNT

at $\approx 25 \mu\text{A}$. High bias I/V characteristics are shown in Fig. 4. Fig. 4a corresponds to an individual SWNT. The saturation current can be extracted from the relation for the electrical resistance $R \equiv V/I$ [15]

$$R = R_0 + V/I_0, \quad (1)$$

where R_0 is a constant and I_0 is the saturation current. The dependence of $R(V)$ versus the bias voltage V is shown in the insets of Fig. 4 with corresponding fits to Eq. 1. Because the saturation current is relatively well defined, its measurement allows to deduce the number of participating CNTs. Whereas Fig. 4a corresponds to a single SWNT, two nanotubes seem to participate in transport in the example shown in Fig. 4b. This result is consistent with the one above and points to the presence of more than one tube. This saturation-current method works for SWNTs but also for multi-wall CNTs [16]. One can therefore not distinguish whether one deals with two tubes in a rope or with one double-wall CNT.

LOW-OHMIC CONTACTS

It is well known that physical phenomena explored by electrical transport measurements (especially at low temperatures) dramatically depend on the transparency between the contacts and the CNT. At low energies, the electronic transport through an ideal metallic single-wall carbon nanotube (SWNT) is governed by four modes (spin included). In the Landauer-Büttiker formalism [17] the conductance can be written as

$$G = T \cdot 4e^2/h, \quad (2)$$

where T is the total transmission probability between source and drain contacts. For low transparent contacts ($T \ll 1$) the CNT forms a quantum dot (QD) which is weakly coupled to the leads. Charge transport is then determined by the sequential tunnelling of single electrons (Coulomb blockade regime). If the transmission probability is increased (for which better contacts are required), higher-order tunnelling processes (so called co-tunnelling) become important which can lead to the appearance of the Kondo effect. This phenomenon was first reported by Nygård *et al.* [18]. At transparencies approaching $T \approx 1$ we enter the regime of ballistic transport where residual backscattering at the contacts leads to Fabry-Perot like resonances [19]. Good contacts with transparencies close to one are indispensable for the exploration of superconductivity [20], multiple Andreev reflection [21] or spin injection [22] in CNTs. Nevertheless, modest progress has been made so far on the control of the contact resistances between CNTs and metal leads. Annealing is one possible route, as proposed by the IBM group [23] and we confirm their results here. We compare in the following Ti, Au and Pd contacts.

Comparison between Ti, Au and Pd contacts

In the ideal case of fully transmissive contacts, a metallic SWNT is expected to have a conductance of $G = 4e^2/h$ (two modes), which corresponds to a two-terminal resistance

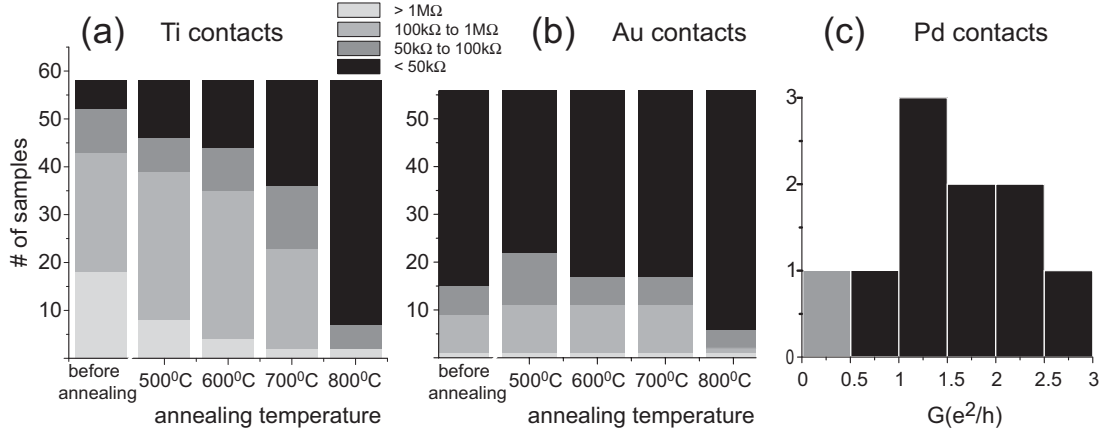


FIGURE 5. Comparison of the two-terminal resistance R at room temperature of CNT devices which were contacted with different metals: (a) Ti, (b) Au and (c) Pd. Post-annealing has been done in vacuum ($< 10^{-5} \text{ mbar}$) in case of Ti and Au. In (a) and (b) the evolution of R for a large number (≈ 55) of samples as a function of annealing temperature is displayed in the form of a histogram. The representation for Pd (c) is different: the conductance $G = 1/R$ of 10 samples are compared, out of which only one has a resistance $R > 50 \text{ k}\Omega$, corresponding to $G < 0.5 e^2/h$.

of $6.5 \text{ k}\Omega$. In case of contacts made by Ti, Ti/Au or Cr on as grown SWNTs, most of the devices show resistances in the range between $100 \text{ k}\Omega$ to $1 \text{ M}\Omega$. In contrast, Au contacts are better, because the measured resistances range typically between $40 \text{ k}\Omega$ and $100 \text{ k}\Omega$. Even for the highest conductive sample the transmission probability is rather small and amounts to only $T \approx 0.16$ (per channel).

To lower the contact resistances we added an annealing step to the process, which was motivated by the work of R. Martel *et al.* [23]. We have performed annealing on more than 50 samples in a vacuum chamber fitted with a heating stage at a back-ground pressure of $< 10^{-5} \text{ mbar}$. The resistance is first recorded on as prepared devices. Then, they are annealed with temperature steps of 100°C for 5 min starting at 500°C . The results for titanium and gold contacts are shown in Fig. 5a and 5b, respectively.

In agreement with previous work [23] we find a pronounced resistance decrease for Ti contacts, if annealed at 800°C . It was suggested by R. Martel *et al.* [23] that the origin of the resistance decrease is the formation of titanium carbide (Ti_xC) at temperatures over 700°C . In contrast to Ti contacts, we do not observe a dramatic change in the sample resistance versus annealing temperature in case of Au contacts. This suggests that unlike Ti on carbon no chemical reactions take place between Au and carbon even at temperatures as large as 800°C . We have also compared annealing in vacuum with annealing in hydrogen within the same temperature window (not shown). The outcome in terms of resistance change is comparable to the vacuum results provided that $T < 700^\circ\text{C}$. At temperatures above $\approx 700^\circ\text{C}$ the majority of the devices display a short to the back-gate. We think that the reducing atmosphere is very effective in partially etching the SiO_2 at these high temperatures.

Finally, we have also studied as-grown Pd contacts, which were recently reported to lead to contacts that are lower ohmic than Au [9]. In our own work (Fig. 5c) we have indeed found independently of Javey *et al.* [9] that palladium makes excellent contacts

to CNTs. There is no need for an additional post-growth treatment [14]. Metallization of CNT devices with Pd is the preferred method, because it yields low-ohmic contacts without an additional annealing step. Careful transport studies of Pd contacted SWNTs show Coulomb blockade, Kondo physics and Fano resonances [14]. The observed resonances suggest that even in nanotubes, which look at first sight ideal, interference with additional transport channels may appear. The only plausible explanation for this observation is the existence of other tubes, hence a bundle or multishell nanotube.

CONCLUSION

Many applications of carbon nanotubes (CNTs) require to reproducibly place and contact single *small* diameter tubes. This is important, for example, for the realization of mechanical resonators [8], for field-effect transistors with reproducible characteristics and for fundamental studies of electron transport. One approach is to start from a powder of CNTs which is obtained, for example, in arc-discharge or laser-evaporation. Because these methods yield bundles of dozens of tubes, individual CNTs can only be obtained by rigorous ultrasonics and separation in an ultracentrifuge in the presence of a surfactant. If the ultrasonic step is too rigorous, the CNTs are cut into short pieces. Spreading and contacting of single tubes is possible. However, one has to bear in mind that these CNTs are covered by a surfactant which is likely to affect the fabrication of low-ohmic contacts. Moreover, the surfactant may carry charge which dopes the CNTs. In contrast to this approach, chemical vapor deposition (CVD) yields tubes in a very direct way immediately on the chip and without a surfactant, which makes this approach very attractive. Whereas a profound comparison of the quality in terms of the number of defects between these two major classes of CNTs is not yet established, the degree of bundling can be compared today. If grown by CVD on a surface at relatively high temperature and with a low catalyst density, apparently single-wall CNTs can be grown, though with a much larger spread in diameter as compared to e.g. the laser method. Although, the tubes appear to be single, as judged from SEM and simple tapping-mode AFM in air, we find in a number of different experiments clear signs for the presence of more than one tube. Measured saturation currents are often larger than the value expected for a single tube. Suspended tubes, even if no bundling is apparent in SEM in the form of branches, do not thermally vibrate as expected for a typical SWNT [8]. And finally, the presence of interference effects in transport (Fano resonances) point to additional transport channels that are likely due to additional shells or tube [14]. The results presented in this work show however, that the number of tubes can be small, e.g. 2-3. This gives hope that with refined catalysts, the controlled production of single tubes should be possible. In addition, we have demonstrated that relatively low-ohmic contacts can be achieved either with Ti, if an additional annealing step is used, or by Au and Pd without any additional treatment. Out of these three materials, Pd yields the best contacts (lowest contact resistance).

ACKNOWLEDGMENTS

We acknowledge contributions and discussions to this work by T. Y. Choi (ETHZ), J. Gobrecht (PSI), and D. Poulikakos (ETHZ). Support by the Swiss National Science Foundation, the NCCR on Nanoscience and the BBW is gratefully acknowledged.

REFERENCES

1. Kong, J., Cassel, A. M., and Dai, H., *Chem. Phys. Lett.*, **292**, 567–574 (1998).
2. Hafner, J. H., Bronikowski, M. J., Azamian, B. R., Nikolaev, P., Rinzler, A. G., Colbert, D. T., Smith, K. A., and Smalley, R. E., *Chem. Phys. Lett.*, **296**, 195–202 (1998).
3. Kong, J., Soh, H. T., Cassel, A. M., Quate, C. F., and Dai, H., *Nature*, **395**, 878–881 (1998).
4. Calibrated massflow controllers were used, except for the large flow rate of methane of 5000 cm³/min, which was adjusted and measured with a floating ball meter calibrated to air. The correction factor for methane is ≈ 1.4 , i.e. the actual flow was 1.4 times larger.
5. Two different substrates are used: Si/SiO₂ or Si/SiO₂/Si₃N₄ heterostructure.
6. Treacy, M. M. J., Ebbesen, T. W., and Gibson, J. M., *Nature*, **381**, 678 (1996).
7. Poncharal, P., Wang, Z. L., Ugarte, D., and Heer, W. A., *Science*, **283**, 1513 (1999).
8. Babić, B., Furer, J., Sahoo, S., Farhangfar, S., and Schönenberger, C., *Nano. Lett.*, **3(11)**, 1577 (2003).
9. Javey, A., Guo, J., Wang, Q., Lundstrom, M., and Dai, H., *Nature*, **424**, 654 (2003).
10. Chromium is used because it could sustain high temperature of CVD process with no apparent diffusion.
11. Tans, S. J., Devoret, M. H., Groeneveld, R. J. A., and Dekker, C., *Nature*, **394**, 761–764 (1998).
12. Bockrath, M., Cobden, D. H., McEuen, P. L., Chopra, N. G., Zettl, A., Thess, A., and Smalley, R. E., *Science*, **275**, 1922–1925 (1997).
13. Nygård, J., Cobden, D., and Lindelof, P. E., *Nature*, **408**, 342 (2000).
14. B. Babić *et al.* (to be published).
15. Yao, Z., Kane, C. L., and Dekker, C., *Phys. Rev. Lett.*, **84**, 2941 (2000).
16. Collins, P. G., Arnold, M. S., and Avouris, P., *Science*, **292**, 706–709 (2001).
17. Büttiker, M., *Quantum Mesoscopic Phenomena and Mesoscopic Devices in Microelectronics*, Kluwer Academic Publishers, New York, 2000, pp. 211–242.
18. Nygård, J., Cobden, D., and Lindelof, P. E., *Nature*, **408**, 342 (2000).
19. Liang, W., Bockrath, M., Bozovic, D., Hafner, J. H., Tinkham, M., and Park, H., *Nature*, **411**, 665–669 (2001).
20. Kasumov, A. Y., Deblock, R., Kociak, M., Reulet, B., Bouchiat, H., Khodos, I. I., Gorbatov, Y. B., Volkov, V. T., Journet, C., and Burghard, M., *Science*, **284**, 1508 (1999).
21. Buitelaar, M. R., Belzig, W., Nussbaumer, T., Babić, B., Bruder, C., and Schönenberger, C., *Phys. Rev. Lett.*, **91**, 057005 (2003).
22. Jensen, A., Nygård, J., and J. Borggreen, *World Scientific*, pp. 33–37 (2003).
23. Martel, R., Derycke, V., Lavoie, C., Appenzeller, J., Chan, K., Tersoff, J., and Avouris, P., *Phys. Rev. Lett.*, **87**, 256805–1 (2001).